JBUON 2021; 26(5): 2040-2052
ISSN: 1107-0625, online ISSN: 2241-6293 • www.jbuon.com
Email: editorial_office@jbuon.com

ORIGINAL ARTICLE

Integrated analysis of hub gene expression in multiple myeloma

Yanping Huang[1], Jinxiong Huang[2], Peng Zhang[3], Jun Luo[1], Peng Cheng[1], Liu Miao[4], Yongrong Lai[1]

[1]Department of Hematology, the First Affiliated Hospital of Guangxi Medical University, Nanning, China. [2]Department of Hematology, Liuzhou People's Hospital Affiliated to Guangxi Medical University, Liuzhou, China. [3]Department of Infection, Liuzhou People's Hospital Affiliated to Guangxi Medical University, Liuzhou, China. [4]Cardiovascular Department, Liuzhou People's Hospital Affiliated to Guangxi Medical University.

Summary

Purpose: *To explore the expression and clinical significance of factors associated with multiple myeloma (MM) and identify new diagnostic markers.*

Methods: *Two gene expression array data sets (GSE6477 and GSE5900) were downloaded and differentially expressed genes (DEGs) in bone marrow from patients with MM and healthy donors analyzed. Kyoto Encyclopedia of Genes and Genomes pathway enrichment and Gene Ontology annotation of DEGs was conducted and a protein-protein interaction network generated. Plasma and bone marrow samples from patients with MM were analyzed for cytokine expression by ELISA and correlations between cytokine levels and clinical indicators evaluated.*

Results: *Of 908 DEGs, 416 were up-regulated and 492 down-regulated. Further, 161 proteins pairs and 21 nodes were detected, and eight hub genes (CXCL2, CXCL8, CXCL12, ELANE, LCN2, CX3CL1, CCL13, and CCL27) screened out. Expression levels of CXCL8, CXCL2, CXCL12, LCN2, and CCL13 were low in CD138⁺ plasma cells, and expression levels of the eight cytokines differed significantly in peripheral blood plasma from patients with MM and healthy controls. ROC curve analysis determined optimal diagnostic thresholds determined for: CCL27 (189 ng/mL), CXCL2 (313 ng/L), CX3CL1 (132 ng/L), CCL13 (235 pg/mL), CXCL8 (884 ng/L), ELANE (50 μg/L), LCN2 (8 μg/L), and CXCL12 (2525 pg/mL).*

Conclusions: *CX3CL1, CCL13, CXCL8, and CXCL12 levels were positively correlated with those of hemoglobin and β2 microglobulin (β2-MG); CCL27 and CXCL2 with β2-MG; and CCL13 and ELANE with white blood cell count and age, respectively. CCL27, CXCL2, and β2-MG levels were associated with MM incidence.*

Key words: *multiple myeloma, array data, integrated analysis, gene ontology annotation, gene expression, Cox proportional hazards regression*

Introduction

Multiple myeloma (MM) is a malignant tumor characterized by abnormal plasma cell (PC) proliferation, with monoclonal immunoglobulin or light chain (M-protein) overproduction. Age, lactate dehydrogenase (LDH) level, cytogenetic profile, International Staging System (ISS) stage, and curative effect are independent prognostic factors for patients with MM [1,2]. The pathogenesis and prognosis of MM have been the focus of considerable clinical research [3-5], and the cytogenetic and genomic characteristics of tumors can reflect their cell biological features and provide important information regarding disease progression and prognosis [5,6].

Corresponding author: Yongrong Lai, MD. Department of Hematology, the First Affiliated Hospital of Guangxi Medical University, 22 Shuangyong Rd, Nanning, Guangxi 530021, China.
Tel: +86013627825835; Email: laiyongrong@263.net
Received: 03/06/2021; Accepted: 27/07/2021

Although there have been advances in the treatment of MM over recent years, the disease remains an incurable malignancy [7]. The evolution from monoclonal gammopathy of unknown significance (MGUS), to smoldering myeloma (SMM), MM is a complex process influenced by genomic instability, epigenetic features, and microenvironmental signaling [5,8]. The bone marrow microenvironment (BMM) is important for the differentiation, migration, proliferation, survival and drug resistance of malignant PC in patients with MM. The BMM contains macrophages, osteoblasts, endothelial cells and mesenchymal cells, which influence the survival and proliferation of MM cells [9]. The interaction between MM cells and the BMM is a research hotspot, and various studies have identified the importance of this relationship in disease pathogenesis and progression [7,10].

Inflammatory cytokines contribute to the initiation and progression of cancer, and cytokines produced by cancer or cancer-related cells (such as immune infiltrating cells) in the tumor microenvironment can support cancer cell growth, as well as potentially inducing epigenetic changes and genomic instability [1,11].

Analysis of databases incorporating genome-scale data on gene expression, protein sequence, gene functional annotation, protein interaction networks and prediction of genes contributing to disease can be based on a single data type or integrate multiple data classes [12], where the latter often provides better prediction accuracy than the former [13]. New risk stratification tools are required to facilitate understanding of MM and optimize treatment. The GEO database is a free source of globally acquired gene sequencing and array-based data [14]. In this study, we analyzed two MM data sets in the GEO database, focusing on cytokine-cytokine receptor interaction. Transcriptional mis-regulation in cancer, cell adhesion molecules (CAMs) and related factors, including, *CXCL8, CXCL2, LCN2, CXCL12, CCL27, CCL13, CX3CL1*, and *ELANE* expression were screened out, and tested in samples from 64 patients with MM, with the aim of determining the expression pattern and functions of these eight cytokines in the context of this disease. Further, correlations of these factors with clinical indicators, including hemoglobin, LDH, and β2 microglobulin (β2-MG) were also analyzed.

Methods

Affymetrix microarray data

Two gene expression profile data sets, GSE6477 and GSE5900, including data from $CD138^+$ PCs selected from bone marrow samples, were analyzed. GSE6477 contained 162 samples, including 15 healthy donors, 22 patients with MGUS, 73 with newly diagnosed MM (NMM), 28 patients with recurrent MM (RMM), and 24 patients with SMM. GSE5900 contained data from 78 samples, including 22 healthy donors, 44 patients with MGUS, and 12 patients with SMM. The Affy package in R was used to transform CEL files into expression value matrices, which were then normalized using RMA methods [15]. Subsequently, the Bioconductor package in R was used to convert probe data to gene expression data. Expression levels detected by some probes were too high or too low for accurate analysis; these were identified as outliers and excluded from further analyses. When multiple probes corresponded to a single gene, the average expression value was used to screen for differentially expressed genes (DEGs). Mean gene expression values were calculated, and the threshold used to define DEGs was $|\log2 \text{ fold-change}| > 1.2$ and adjusted $p < 0.05$.

Gene ontology (GO) and pathway enrichment analyses

Database for Annotation, Visualization and Integrated Discovery (DAVID; version 6.8) [16] was used to identify GO functions and pathways enriched for specific DEGs in the Kyoto Encyclopedia of Genes and Genomes (KEGG) (http://www.genome.ad.jp/kegg/) [17] and GO (http://www.geneontology.org) [18] databases, along with the R package, Goplot [15], with an adjusted p value threshold of < 0.05.

Construction of a protein-protein interaction (PPI) network

The interactive gene retrieval tool database, STRING (V10.5; https://string-db.org/) [19] is a useful platform for studying interactions between experimentally evaluated and predicted proteins. Co-expression experiments, co-occurrence, gene fusion, and neighborhood analysis were conducted using Cytoscape (version 3.60) [20]. Interactions between protein pairs in the database were comprehensively scored. To detect correlations between key genes in the network and potential PPIs, DEGs were mapped to the data, with the critical value set at a combined score > 6. Degree was used to describe the meaning of protein nodes in the network. These three protocols were all processed using the R software package, igraph version 4.0.1. [21].

Module analysis

Protein networks [22], such as network modules, contain useful information about the biological functions of biomolecules. Prominent clustering modules were determined using the Cytoscape software package, molecular complex detection (MCODE). Next, the DAVID online tool was used to analyze KEGG pathways enriched for DEGs between modules. Cut-off values of count ≥ 2 and EASE ≤ 0.05, and an MCODE score > 6 were used as threshold values for follow-up analysis.

Collection of clinical specimens

Bone marrow and peripheral plasma samples were collected from 64 patients newly diagnosed with MM from March 2019 to September 2020, including 39 males and 25 females, aged 45-86 years (mean 60.48).

According to the ISS, 14 patients had Phase I, 23 patients Phase II, and 27 Phase III disease. Further, 25 cases were complicated with pneumonia, 26 with cardiovascular disease and 11 with diabetes. FISH analysis showed that four cases had t (11,14) and four had t (4,14) translocations; four had deletion of 14q32, six deletion of 1q21, two of *IgH*, three *TP53*, and one case each had del (20q-), t (14,20), and del (7p-) mutations; four of these patients had dual mutations. Peripheral plasma samples from 21 patients with lumbar disc herniation and lumbar hyperosteogeny admitted to the Department of Spine and Orthopedics were used as the control group. Patients with autoimmune diseases were excluded. Samples were centrifuged at 2000 × g and supernatants collected and frozen at –80°C. All patients signed informed consent.

Hub gene determination in bone marrow and peripheral blood plasma samples

ELISA kits (Shanghai Hengyuan Biological Co., Ltd., Shanghai, China) were used to verify the expression of various cytokines in 64 patients newly diagnosed with MM and 21 controls.

Statistics

SPSS 21.0 package (SPSS Inc. Chicago, IL, USA) was used for statistical analyses. Chi square was used to compare differences between groups. Continuous data are presented as mean ± SD. Nominal significance was considered for raw p values<0.05. Univariate analysis was used to determine the association of clinical variables and genes with myeloma endpoints.

Results

Identification of DEGs

Analysis of gene expression profile data from GSE5900 and GSE6477 identified a total of 32586 expression probes. DEGs were defined as those with |log 2 (fold change) | ≥ 1.2 and an adjusted p value < 0.05; 908 DEGs meeting these criteria were obtained, of which 394 were screened from GSE5900 (253 up-regulated and 141 down-regulated) and 514 from GSE6477 (163 up-regulated and 351 down-regulated). Heat maps and volcano plots showing the distribution of DEGs from each dataset are presented in Figure 1.

Analysis of gene ontology functions and KEGG pathways enriched for DEGs

To identify disease-related genes, 30 pathways were identified by screening 718 GO functional pathways for DEG enrichment, including lymphocyte regulation, neutrophil activation, neutrophil degranulation, lymphocyte proliferation, and humoral immune response. The DAVID tool (version 6.8) was also used for the KEGG pathway analysis of screened DEGs, which were enriched in 10 KEGG pathways, including cytokine-cytokine receptor interaction, transcriptional mis-regulation in cancer, CAMs, hematopoietic cell lineage, systemic lupus erythematosus, *Staphylococcus aureus* infection, melanoma, malaria, asthma, and thyroid cancer. Enriched DO pathways included connective tissue cancer, obstruction lung disease, bone cancer, osteosarcoma, dermatitis, demyelinating disease, multiple sclerosis, myeloid leukemia, vasculitis, and leukocyte disease (Figure 2).

Protein-protein interaction (PPI) network construction

Using STRING and PPI analysis, 161 pairs of proteins, 21 nodes, and 8 highly DEGs were screened out, including CXCL2 (degree=37), CXCL8 (degree=103), CXCL12 (degree=66), CCL13 (degree=25), CCL27 (degree=31), CXCL1 (degree=31), ELANE (degree=48), and LCN2 (degree=37) (Figure 3; Table 1).

Expression of screened genes in CD138⁺ PCs

CD138⁺ PC mRNA data from both the GSE5900 and GSE6477 data sets was analyzed. In GSE5900, none of the screened genes were up-regulated in MM compared with healthy controls, while *CXCL8, CXCl2, LCN2, CXCL12, CCL27,* and *CCL13*

Table 1. The significant modules identified from the protein-protein interaction network using the molecular complex detection method with a score > 14

Gene	*MCODE_Score*	*MCODE_Cluster*	*Degree*
ELANE	14	Cluster 1	48
CXCL8	17	Cluster 1	103
DEFA4	14	Cluster 1	24
CXCL2	17	Cluster 1	37
LCN2	14	Cluster 1	37
ANXA1	17	Cluster 1	36
FPR3	17	Cluster 1	28
CXCL12	17	Cluster 1	66
CX_3CL1	17	Cluster 1	31
CCL13	17	Cluster 1	25
C5AR1	17	Cluster 1	39
GRM2	17	Cluster 1	23
DRD4	17	Cluster 1	24
CCL27	17	Cluster 1	31
HTR1D	17	Cluster 1	18
PYY	17	Cluster 1	23
MCHR1	17	Cluster 1	29
GPR183	17	Cluster 1	26
OXGR1	17	Cluster 1	17
P2RY13	17	Cluster 1	24
HCAR3	17	Cluster 1	18

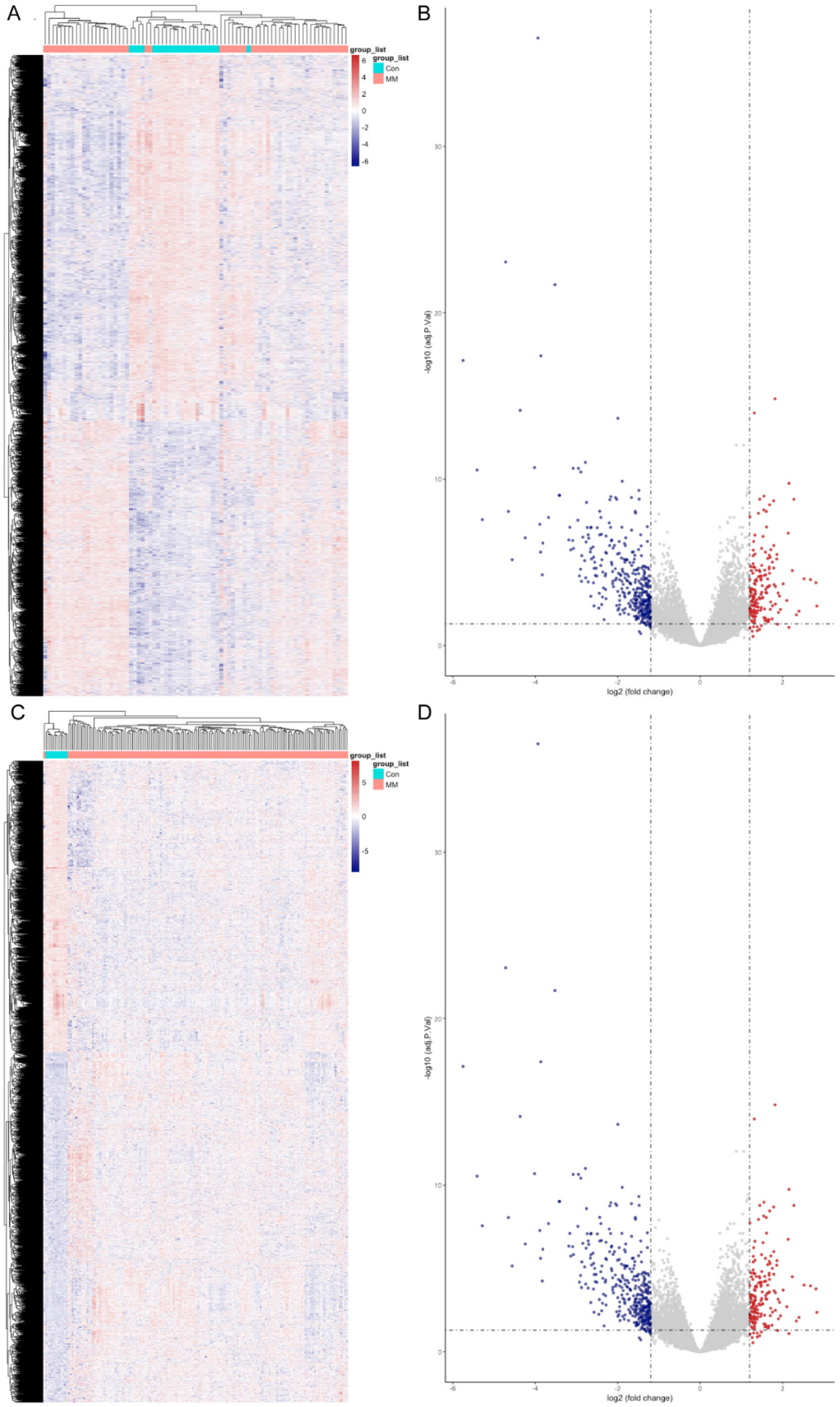

Figure 1. Heat map of differentially expressed genes. The depth of color reflects the level of differential expression (log fold-change). The two vertical lines indicated the 2-fold change boundaries and the horizontal line indicates the statistical significance threshold (Adj-p< 0.05). Genes with a fold change ≥1.2 and statistical significance are indicated by red dots (up-regulated) and blue dots (down-regulated). **A:** GSE5900 heat map. **B:** GSE5900 volcano plot. **C:** GSE6477 heat map. **D:** GSE6477 volcano plot.

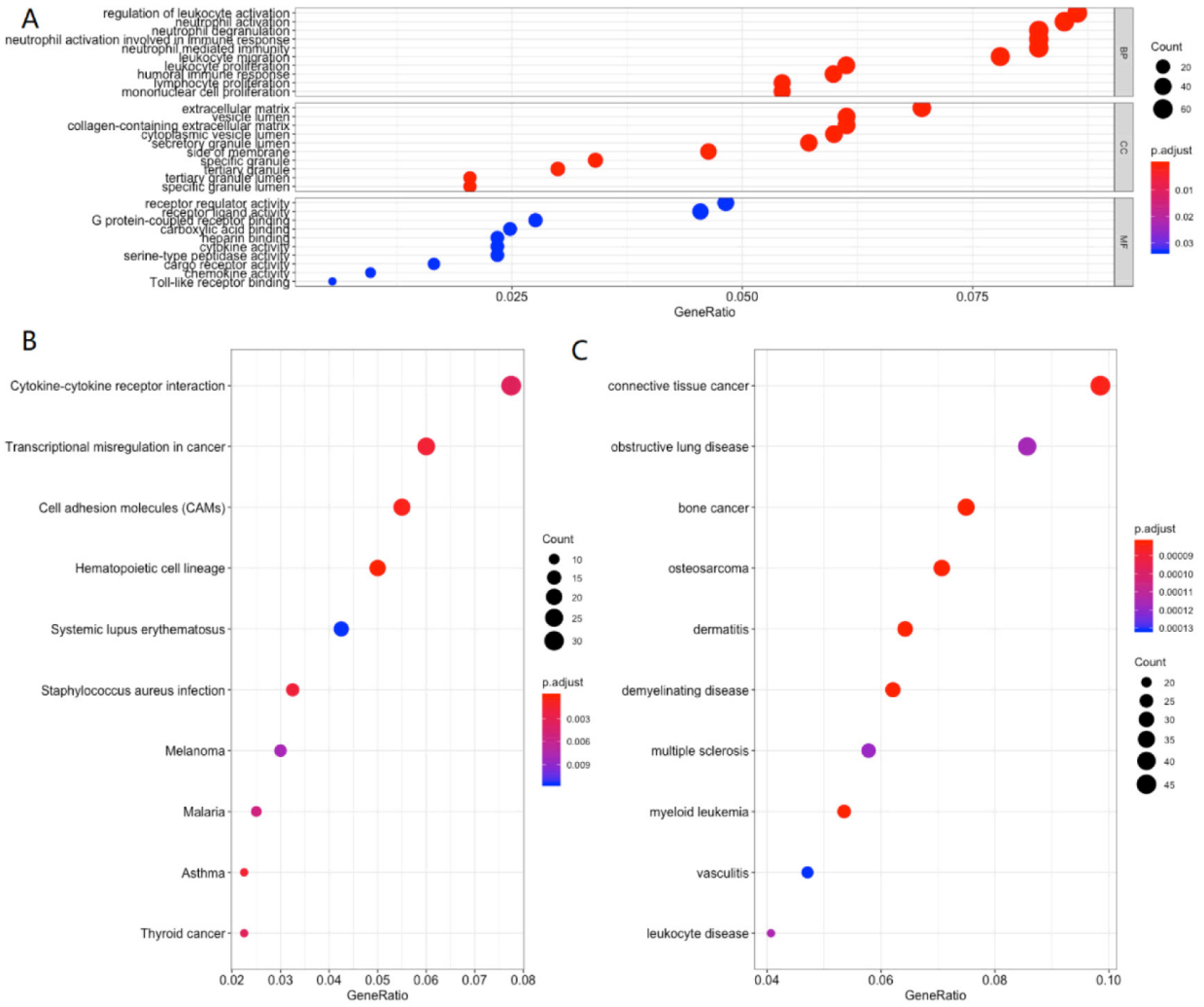

Figure 2. Gene ontology terms and pathways enriched for differentially expressed genes (DEGs). The size of dots corresponds to the DEG count and the color represents the level of significance of the term, with larger dots representing higher counts. **A:** GO pathway. **B:** KEGG pathway. **C:** DO pathway.

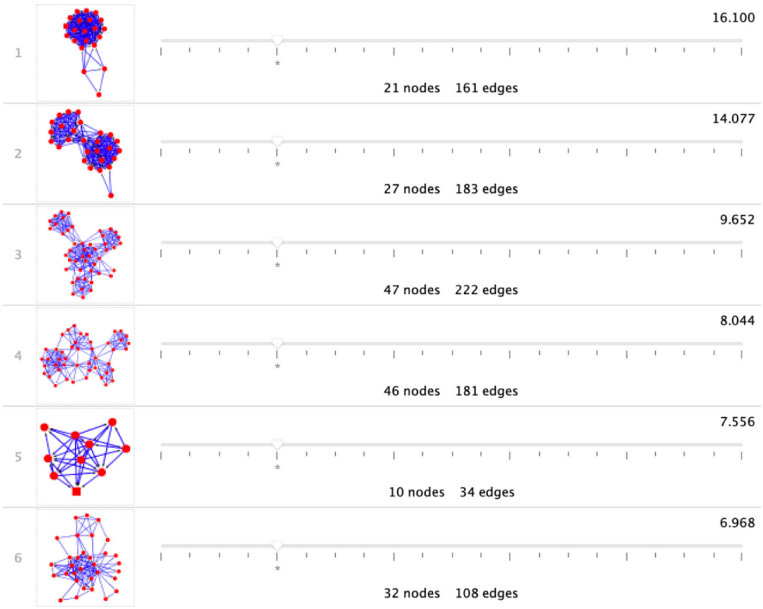

Figure 3. Topological properties of the PPI network. Using STRING and PPI analysis, and choosing 161 pairs of proteins, 21 nodes and 8 highly differentially expressed genes were screened out.

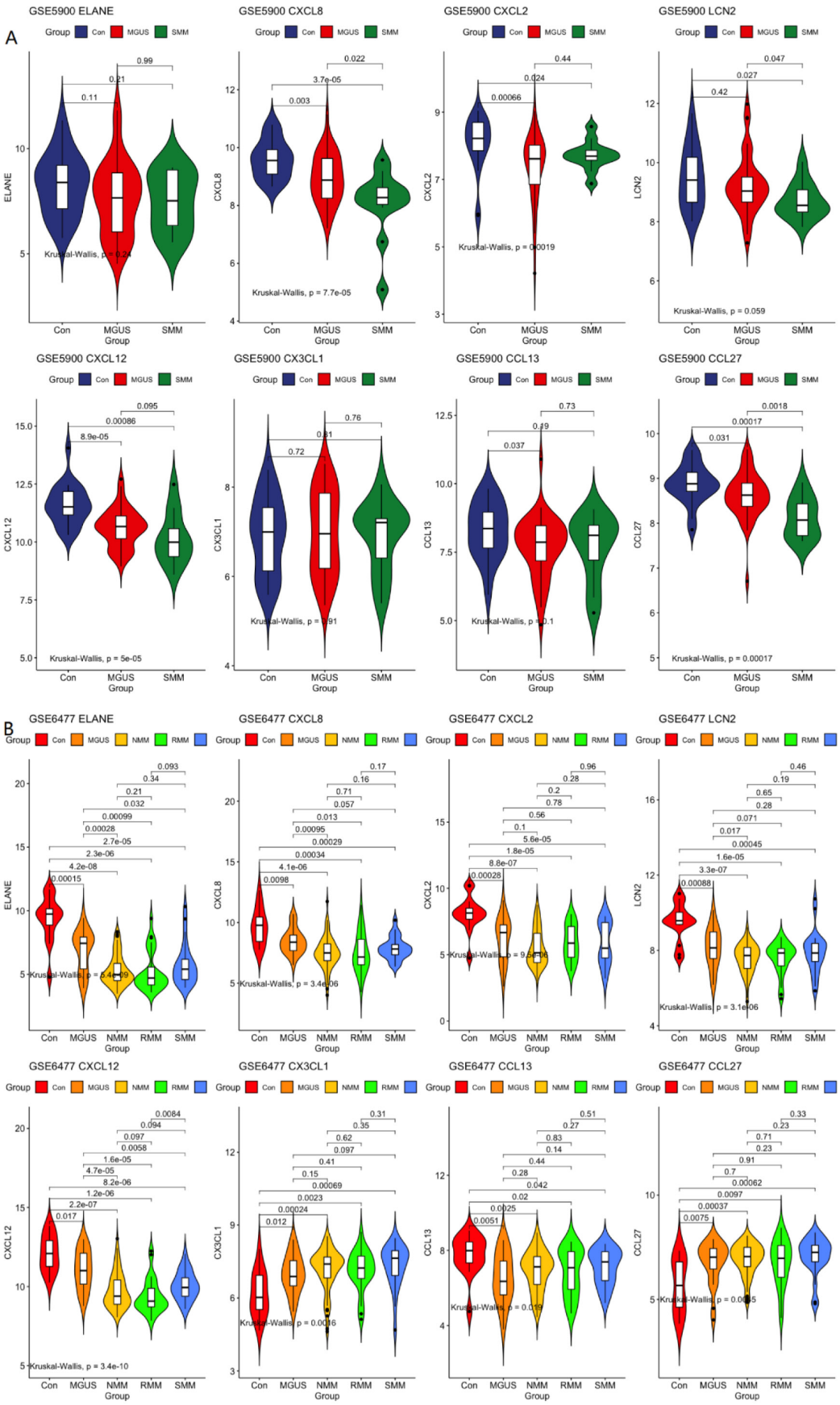

Figure 4. Expression profiles of hub genes generated from microarray data. Eight differentially expressed genes, *CXCL2, CXCL8, CXCL12, CCL13, CCL27, CX3CL1, ELANE,* and *LCN2*, were detected in GSE5900 and GSE6477. Comparison of Control, MGUS, and SMM groups in GSE900. Comparison of Control, MGUS, NMM, RMM, and SMM groups in GSE6477. **A:** GSE5900. **B:** GSE6477.

expression levels were downregulated, and those of *CX3CL1* and *ELANE* did not differ significantly. In *GSE6477*, *ELANE*, *CXCL8*, *CXCL2*, *LCN2*, *CXCL12*, and *CCL13* levels were down-regulated MM compared with controls, while those of *CX3CL1* and *CCL27* were upregulated in both data sets. Hence, expression levels of *CXCL8*, *CXCL2*, *CXCL12*, *LCN2*, and *CCL13* were decreased in both datasets, while that of *CCL27* was upregulated (Figure 4).

Expression of hub genes in bone marrow and plasma

CXCL2, *CXCL8*, *CXCL12*, *ELANE*, *LCN2*, *CX3CL1*, *CCL13*, and *CCL27* expression levels were assessed in bone marrow and peripheral blood plasma samples. Levels in peripheral blood from patients with MM differed significantly from those from healthy controls ($p < 0.05$); however, there was no significant difference between MM bone marrow and MM peripheral plasma samples (Table 2).

Table 2. Changes of cytokines in bone marrow and plasma of MM

Gene	*group*	$\overline{x}\pm s$	*test-statistic*	*p value*
CCL27 (pg/ml)	Bone marrow	207.81±19.97[a]	7.165	0.000
	plasma	199.89±22.34[b]	5.949	0.000
	control	166.70±17.50		
CX3CL1 (ng/L)	Bone marrow	169.88±29.66[a]	6.008	0.000
	plasma	163.28±28.03[b]	5.956	0.000
	control	121.18±22.87		
CXCL2 (ng/L)	Bone marrow	329.16±36.79[a]	5.179	0.000
	plasma	318.81±39.46[b]	4.392	0.000
	control	275.66±30.50		
CCL13 (pg/ml)	Bone marrow	261.41±36.60[a]	4.853	0.000
	plasma	267.67±33.91[b]	6.208	0.000
	control	218.70±17.30		
CXCL8 (ng/ml)	Bone marrow	1003.09±158.43[a]	4.954	0.000
	plasma	1011.26±173.53[b]	5.221	0.000
	control	791.76±117.16		
ELANE (ug/L)	Bone marrow	50.92±6.94[a]	2.652	0.011
	plasma	52.96±8.46[b]	3.53	0.001
	control	45.65±6.03		
LCN2 (ug/L)	Bone marrow	8.09±1.11[a]	4.065	0.000
	plasma	7.99±1.02[b]	4.297	0.000
	control	6.92±0.71		
CXCL12 (pg/ml)	Bone marrow	2678.49±452.02[a]	5.875	0.000
	plasma	2874.02±476.21[b]	7.759	0.000
	control	1994.0±290.48		

Note: 'a' is the comparison between the bone marrow group of MM patients and the normal peripheral blood group; 'b' is the peripheral blood group of MM patients compared with the normal peripheral blood group

Table 3. Area under ROC curve of each cytokine

Test result variable	*Area*	*Standard error.a*	*Sig.b*	*95% CI*	
				The lower limit	*ceiling*
CCL27(pg/ml)	0.898	0.035	0.000	0.829	0.967
CXCL2(ng/L)	0.832	0.047	0.000	0.741	0.924
CX3CL1(ng/L)	0.879	0.041	0.000	0.799	0.960
CCL13(pg/ml)	0.892	0.035	0.000	0.824	0.960
CXCL8(ng/L)	0.850	0.043	0.000	0.765	0.935
ELANE(ug/L)	0.737	0.055	0.001	0.629	0.846
LCN2(ug/L)	0.792	0.049	0.000	0.696	0.888
CXCL12(pg/ml)	0.938	0.025	0.000	0.890	0.987

Table 4. The optimal diagnostic threshold of each cytokine

Gene	*diagnostic threshold*	*sensitivity*	*1- Specificity*	*Specificity*	*Youden's Index*
CCL27	189.355 (ng/ml)	0.797	0.0476	0.952	1.749
CXCL2	313.430 (ng/L)	0.625	0.0476	0.952	1.577
CX3CL1	132.675 (ng/L)	0.875	0.286	0.714	1.589
CCL13	235.350 (pg/ml)	0.8125	0.143	0.857	1.670
CXCL8	884.205 (ng/L)	0.781	0.143	0.857	1.638
ELANE	50.34 (ug/L)	0.625	0.190	0.810	1.435
LCN2	7.770 (ug/L)	0.095	0.095	0.905	1.545
CXCL12	2525.495 (pg/ml)	0.750	0.000	1.000	1.750

Table 5. Expression of cytokines between myeloma and normal groups

Gene	*group*	*Myeloma /case*	*Control/case*	x^2	*p value*
CCL27	≥189.355(ng/ml)	49	1	30.755	0.000
	<189.355(ng/ml)	15	20		
CXCL2	≥313.430(ng/L)	44	1	23.481	0.000
	<313.430(ng/L)	20	20		
CX3CL1	≥132.675(ng/L)	56	6	27.820	0.000
	<132.675(ng/L)	8	15		
CCL13	≥235.350(pg/ml)	46	3	19.184	0.000
	<235.350(pg/ml)	18	18		
CXCL8	≥884.205(ng/L)	48	3	21.822	0.000
	<884.205(ng/L)	16	18		
ELANE	≥50.34(ug/L)	37	4	8.027	0.005
	<50.34(ug/L)	27	17		
LCN2	≥7.770(ug/L)	40	2	15.697	0.000
	<7.770(ug/L)	24	19		
CXCL12	≥2525.495(pg/ml)	41	0	23.487	0.000
	<2525.495(pg/ml)	23	21		
age	<60	33	16	3.928	0.047
	≥60	31	5		
sex	male	39	14	0.221	0.638
	female	25	7		
White blood cells	$<4\times10^9$/L	24	3	3.931	0.047
	$\geq4\times10^9$/L	40	18		
LDH	≥245 U/L	43	2	21.103	0.000
	<245 U/L	21	19		
Ca^{2+}	≥3.0 mmoL/L	10	0	2.366	0.124
	<3.0 mmoL/L	54	21		
Cr	≥176.8 mmol/L	46	2	25.007	0.000
	<176.8 mmol/L	18	19		
Hb	<100 g/L	41	5	10.318	0.001
	≥100 g/L	23	16		
β2-MG	<3.5 mg/L	14	20	35.459	0.000
	≥3.5 mg/L	50	1		
Serum globulin	Elevated	45	3	20.191	0.000
	Nomal	19	18		

Prediction of optimal diagnostic thresholds for each index

Next, ROC curve analysis was used to verify the specificity and sensitivity of each identified indicator. The optimal diagnostic thresholds determined for *CCL27, CXCL2, CX3CL1, CCL13, CXCL8, ELANE, LCN2,* and *CXCL12* were 189 ng/mL, 313 ng/L, 132 ng/L, 235 pg/mL, 884 ng/L, 50 μg/L, 7 μg/L, and 2525 pg/mL, respectively. Area under the ROC curve values for each cytokine were 0.967, 0.924, 0.960, 0.960, 0.935, 0.846, 0.888, and 0.987, respectively (Table 3, Table 4 and Figure 5). Taking each threshold as the boundary, differences in each index between the myeloma and healthy groups were compared. Levels of each index were significantly higher in myeloma than control samples, as were those of serum LDH, Cr, Hb, β2-MG, and globulin; the differences were statistically significant (Table 5).

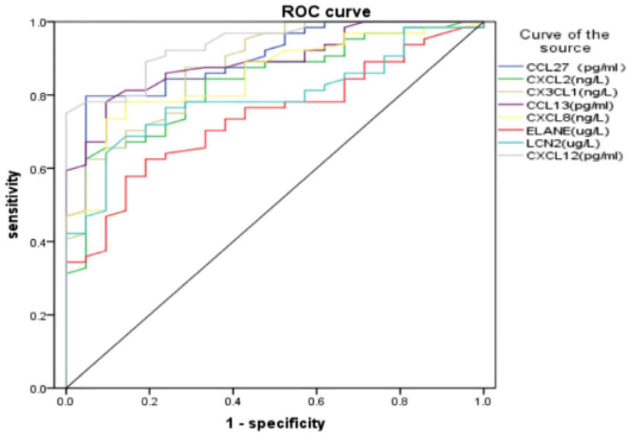

Figure 5. ROC curve analyses of each cytokine. The y-axis indicates the sensitivity and the x-axis represents 1- specificity.

Correlations between hub gene expression levels and clinical indicators

CX3CL1, CCL13, CXCL8, and *CXCL12* levels were positively correlated with those of hemoglobin and β2-MG; CCL27 and CXCL2 levels were only correlated with β2-MG level; while CCL13 was associated with white blood cell count. No hub genes correlated with the ratio of primitive and immature PCs in bone marrow or LDH were detected. Multi-

Table 6. The correlation between the test variables and clinical indicators

Correlation coefficient	*CCL27*	*CX3CL1*	*CXCL2*	*CCL13*	*CXCL8*	*ELANE*	*LCN2*	*CXCL12*
Age								
r	0.007	-0.127	0.011	0.185	0.045	0.274	0.006	0.044
p value	0.948	0.247	0.919	0.090	0.679	0.011	0.959	0.689
WB								
r	-0.120	-0.025	-0.180	-0.349	-0.185	-0.122	-0.067	-0.123
p value	0.275	0.823	0.099	0.001	0.090	0.265	0.540	0.261
Hb								
r	-0.189	-0.295	-0.400	-0.275	-0.361	-0.171	0.009	-0.315
p-value	0.083	0.006	0.000	0.011	0.001	0.117	0.938	0.003
Plt								
r	-0.012	0.06	-0.030	-0.112	-0.149	-0.178	-0.061	0.069
p value	0.927	0.635	0.812	0.380	0.240	0.160	0.631	0.590
Cr								
r	-0.008	0.113	-0.030	-0.153	-0.101	-0.024	0.084	-0.093
p value	0.945	0.310	0.789	0.166	0.362	0.828	0.449	0.402
LDH								
r	0.200	0.162	0.053	-0.071	-0.036	-0.029	0.026	0.123
p value	0.067	0.139	0.627	0.520	0.742	0.795	0.814	0.264
β2-MG								
r	0.421	0.526	0.359	0.244	0.457	0.184	0.206	0.410
p value	0.000	0.000	0.001	0.029	0.000	0.102	0.066	0.000
Homocysteine								
r	0.421	0.181	0.132	-0.131	-0.257	0.045	0.089	-0.041
p value	0.000	0.204	0.362	0.363	0.071	0.755	0.537	0.776
Percentage of PC								
r	0.173	0.021	0.156	0.094	-0.077	0.018	-0.249	-0.059
p-value	0.344	0.908	0.394	0.610	0.676	0.923	0.170	0.750

Percentage of PC, Percentage of primary and young plasma cells

Table 7. Multivariate logistic regression analysis of multiple myeloma diagnosis

Independent variable	*Regression coefficient*	*Standard deviation*	*Wald-value*	*OR(95%CI)*	*p value*
CCL27	4.691	1.443	10.570	108.9 (6.4~1843.0)	0.001
CXCL2	3.478	1.513	5.288	32.4 (1.67~628.4)	0.021
β2-MG	4.111	1.445	8.090	61.0 (3.59~1037.4)	0.004

variate analysis demonstrated that CCL27, CXCL2, and β2-MG levels were associated with myeloma incidence (Table 6, Table 7).

Discussion

Significant improvements in microarray expression data have facilitated identification of abnormally expressed genes, which can help in disease diagnosis and treatment; however, results based on microarray data are not always repeatable and can be error prone. Hence, it is advisable to eliminate false positives by analyzing various data sets from experiments designed in parallel [23,24]. In this study, we investigated the expression and potential biological functions of inflammatory cytokines in MM using bioinformatics tools.

Chemokines have recently been recognized as tumor markers [14,25], and have important roles in tumor occurrence and progression. Cytokines and chemokines produced by immune-related cells in the tumor microenvironment can induce epigenetic changes and genomic instability, leading to tumor cell growth [26,27]. Myeloma cell proliferation and metastasis, and PC in the BMM are closely associated with bone marrow stromal cells, including osteoblasts, endothelial cells, bone marrow mesenchymal stem cells, hematopoietic cells, and fat cells, which release cell chemotactic factors that can induce resorption of mature osteoclasts and bone [14,28]. By analyzing myeloma gene expression profile data, Botta et al. [28] found that expression of the inflammatory cytokines, *IL2, IL8, IL10, TNF, TGFB1,* and *VEGFA*, differed significantly at various stages of myeloma, and had independent predictive value for disease prognosis; high levels of *IFNG, IL2,* and *CCL2* expression were associated with good prognosis, while high *CCL3* or *VEGFA* expression was associated with poor survival.

In this study, we combined two different myeloma datasets, GSE5900 and GSE6477 and analyzed GO enrichment, KEGG pathways, and PPI networks and modules, to identify eight genes (*CCL27, CXCL2, CX3CL1, CCL13, CXCL8, ELANE, LCN2,* and *CXCL12*), with significantly differential expression between patients and controls. In both data sets, significant differences were observed between patients with MM and healthy controls, with different expression levels detected according to disease stage. In the GSE5900 data set, levels of *CXCL2, CXCL8, CXCL12, CCL27,* and *LCN2* were decreased in the MGUS and SMM groups compared with healthy controls, while *ELANE, CX3CL1,* and *CCL3* levels did not differ significantly from those in the healthy control group. In the GSE6477 data set, levels of *CXCL2, CXCL8, CXCL12, LCN2, ELANE,* and *CCL13* were significantly lower in the MGUS, NMM, RMM, and SMM groups than in healthy controls, while those of *CX3CL1* and *CCL27* were higher. $CD138^+$ PC were analyzed in both datasets. Except for *CXCL2, CXCL8, CXCL12,* and *LCN2*, levels of which were lower in patients than controls in both datasets, the expression levels of other cytokines were not consistent between the two datasets. Based on the results of KEGG/GO analysis, these cytokines may be involved in cell adhesion, transcriptional dysregulation in cancer, cytokine receptor interaction, and hematopoietic cell lineage signaling pathways, among other functions, and have specific roles in hematopoietic system diseases, including myeloma, bone tumors, and MM.

To validate the identified changes of cytokine expression, we collected samples from 64 cases clinically diagnosed with MM [1]. Bone marrow pulp and plasma from patients were examined for changes in various indicators, and we found that levels of *CXCL2, CXCL8, CXCL12, LCN2, ELNAE, CCL13, CX3CL1,* and *CCL27* were significantly higher in MM bone marrow and plasma samples than those in healthy peripheral blood. These results indicate that cytokine secretion is elevated in MM; however, the reason for these observed increases remains unclear.

Bone marrow stromal cell-derived interleukin-8 (IL-8/CXCL8) affects many stages of tumor progression, including survival, proliferation, invasion, and angiogenesis [24]. In this study, we found that *CXCL8* was decreased in myeloma $CD138^+$ PCs, while levels were increased in plasma and bone marrow, suggesting that *CXCL8* may be secreted by bone marrow stromal cells, rather than from bone marrow PCs. Myeloma cell exosomes can promote *CXCL8* release by mesenchymal stem cells through activation of the endothelial growth factor path-

way, thus indirectly inducing osteoclast generation [29]. Immature B cells can also secrete *CXCL8* [30]. Increased *CXCL8* expression in PC tumors is associated with bone metastasis [31], and fibroblasts can also mediate angiogenesis through secretion of *CXCL8* and *CCL2* (MCP-1) [26].

CXCL12 is an important target for inhibiting systemic MM cell migration [32], and a key regulator of the tumor microenvironment, which influences various oncogenic processes, including angiogenesis, as well as promoting tumor cell migration and adhesion to stromal cells [33]. *CXCL12* is secreted by several cell types in the bone marrow, including osteoclasts and endothelial cells, and mediates bone metastasis [31,33]. The CXCL12/CXCR4 signaling pathway functions in tumor cell metastasis and invasion [34,35], and neutralization of *CXCL12* inhibits homing and growth of myeloma cells [33].

ELANE is another member of the CXCL protein superfamily that is mainly produced by neutrophils and enhances antimicrobial activity in an autocrine manner [36]; however, whether this process participates in myeloma development remains unclear. Lentini et al. [37] found that autosomal dominant *ELANE* mutation causes severe congenital neutropenia (SCN). As a proto-oncogene encoded protein, ELANE promotes angiogenesis and plays an important role in tumor genesis, development, and metastasis [38], as well as inhibiting osteoblastic differentiation by down-regulating the ERK1/2 signaling pathway [39].

CX3CL1 is expressed on endothelial and stromal cells in the bone marrow and can be upregulated by tumor necrosis factor (TNFα) in endothelial cells; primary $CD138^+$ cells do not express CX3CL1. Levels of BM CX3CL1 are significantly increased in patients with MM relative to those with SMM and MGUS, and contribute to bone metastasis and angiogenesis in patients with MM [40,41].

CC chemokines are a subfamily comprising 27 chemotactic cytokines, which mediate intercellular communication [42,43]. One of the most important functions of chemotactic cytokines is to recruit monocytes to sites of inflammatory response [44], and they also have crucial roles in the tumor microenvironment [44-46]. There are no reports of the importance of CCL13 in cancer; however, this chemokine may increase apoptosis and can lead to development of drug resistance in tumors [47,48]. Further, CCL27 and CCL28 signaling through CCR10 may cooperate with inflammatory mediators and VEGF-D during tumor lymphangiogenesis [42].

Lipocalin-2 (LCN2) binds covalently to the gelatinase enzyme under conditions of ischemia/hypoxia, stress, and damage, and can be generated in renal tubular epithelial cells; therefore, LCN2 is regarded as a sensitive marker of kidney damage. In MM, urine LCN2 levels are associated with early acute kidney injury and can be used as an early marker of renal function injury [49].

In this study, we used ROC curves to evaluate the specificity and sensitivity of each marker, and determined optimal diagnostic thresholds for CCL27, CXCL2, CX3CL1, CCL13, CXCL8, ELANE, LCN2, and CXCL12 of 189 ng/mL, 313 ng/L, 132 ng/L, 235 pg/mL, 884 ng/L, 50 μg/L, 8 μg/L, and 2525 pg/mL, respectively. Based on these thresholds, comparison of these indices in patients with MM and controls demonstrated that levels of each factor were clearly higher in patients. Further, CCL27, CXCL2, CX3CL1, CCL13, CXCL8, and CXCL12 levels were positively correlated with those of β2-MG. Nevertheless, we did not identify any hub genes correlated with the ratio of primitive and immature PCs in bone marrow or LDH, likely because the study was underpowered due to the small number of cases. No analysis of correlations between cytokines and gene mutations was conducted. We found that high levels of CCL27, CXCL2, and β2-MG are associated with MM incidence. Based on the results of KEGG/GO analysis, these cytokines may be involved in cell adhesion, transcriptional dysregulation in cancer, cytokine receptor interaction, and hematopoietic cell lineage signaling pathways, and these possibilities will be explored in our future research.

This study has certain limitations: the sample size was small, therefore, further studies of molecular pathogenesis and large-scale validation with clinical tumor specimens are required.

Conclusions

Two MM microarray datasets from the GEO series were systematically analyzed in this study. Based on expression levels, enriched GO, KEGG, and DO pathways, and protein-protein interaction analyses, eight genes *(CCL27, CXCL2, CX3CL1, CCL13, CXCL8, ELANE, LCN2, CXCL12)* were found to be expressed at lower levels in MM $CD138^+$ cells; however, they were clearly present at higher levels in patient bone marrow and blood plasma in MM than in controls. *CCL27, CXCL2,* and *β2-MG* levels were associated with MM incidence. The underlying mechanisms may involve lymphocyte regulation, neutrophil activation, neutrophil degranulation, lymphocyte proliferation, and humoral immune response interaction. Our findings provide potential novel biomarkers for early diagnosis of MM.

Conflict of interests

The authors declare no conflict of interests.

References

1. Rajkumar SV, Kumar S. Multiple Myeloma: Diagnosis and Treatment. Mayo Clin Proc 2016;91:101-19.
2. Miannay B, Minvielle S, Roux O et al. Logic programming reveals alteration of key transcription factors in multiple myeloma. Sci Rep 2017;7:9257.
3. M LBA, M ES. CIP2A expression in Bortezomib-treated multiple myeloma. JBUON 2020;25:395-400.
4. Agnelli L, Bisognin A, Todoerti K et al. Expanding the repertoire of miRNAs and miRNA-offset RNAs expressed in multiple myeloma by small RNA deep sequencing. Blood Cancer J 2019;9:21.
5. Went M, Sud A, Speedy H et al. Genetic correlation between multiple myeloma and chronic lymphocytic leukaemia provides evidence for shared aetiology. Blood Cancer J 2018;9:1.
6. Mikhael JR, Dingli D, Roy V et al. Management of newly diagnosed symptomatic multiple myeloma: updated Mayo Stratification of Myeloma and Risk-Adapted Therapy (mSMART) consensus guidelines 2013. Mayo Clin Proc 2013;88:360-76.
7. Zheng Y, Shen H, Xu L et al. Monoclonal Antibodies versus Histone Deacetylase Inhibitors in Combination with Bortezomib or Lenalidomide plus Dexamethasone for the Treatment of Relapsed or Refractory Multiple Myeloma: An Indirect-Comparison Meta-Analysis of Randomized Controlled Trials. J Immunol Res 2018;2018:7646913.
8. Egan JB, Shi CX, Tembe W et al. Whole-genome sequencing of multiple myeloma from diagnosis to plasma cell leukemia reveals genomic initiating events, evolution, and clonal tides. Blood 2012;120:1060-6.
9. Appelmann I, Rillahan CD, de Stanchina E et al. Janus kinase inhibition by ruxolitinib extends dasatinib- and dexamethasone-induced remissions in a mouse model of Ph+ ALL. Blood 2015;125:1444-51.
10. Lopez-Corral L, Corchete LA, Sarasquete ME et al. Transcriptome analysis reveals molecular profiles associated with evolving steps of monoclonal gammopathies. Haematologica 2014;99:1365-72.
11. Miao L, Yin RX, Huang F, Yang S, Chen WX, Wu JZ. Integrated analysis of gene expression changes associated with coronary artery disease. Lipids Health Dis 2019;18:92.
12. Clough E, Barrett T. The Gene Expression Omnibus Database. Methods Mol Biol 2016;1418:93-110.
13. Ahmadzadeh A, Kast RE, Ketabchi N et al. Regulatory effect of chemokines in bone marrow niche. Cell Tissue Res 2015;361:401-10.
14. Tencerova M, Kassem M. The Bone Marrow-Derived Stromal Cells: Commitment and Regulation of Adipogenesis. Front Endocrinol (Lausanne) 2016;7:127.
15. Walter W, Sanchez-Cabo F, Ricote M. GOplot: an R package for visually combining expression data with functional analysis. Bioinformatics 2015;31:2912-4.
16. Huang DW, Sherman BT, Lempicki RA. Systematic and integrative analysis of large gene lists using DAVID bioinformatics resources. Nat Protoc 2009;4:44-57.
17. Kanehisa M, Furumichi M, Tanabe M, Sato Y, Morishima K. KEGG: new perspectives on genomes, pathways, diseases and drugs. Nucleic Acids Res 2017;45:D353-61.
18. Hulsegge I, Kommadath A, Smits MA. Globaltest and GOEAST: two different approaches for Gene Ontology analysis. BMC Proc 2009;3 Suppl 4:S10.
19. Szklarczyk D, Franceschini A, Wyder S et al. STRING v10: protein-protein interaction networks, integrated over the tree of life. Nucleic Acids Res 2015;43:D447-52.
20. Shannon P, Markiel A, Ozier O et al. Cytoscape: a software environment for integrated models of biomolecular interaction networks. Genome Res 2003;13:2498-504.
21. Gustavsen JA, Pai S, Isserlin R, Demchak B, Pico AR. RCy3: Network biology using Cytoscape from within R. F1000 Res 2019;8:1774.
22. Ahmed H, Howton TC, Sun Y, Weinberger N, Belkhadir Y, Mukhtar MS. Network biology discovers pathogen contact points in host protein-protein interactomes. Nat Commun 2018;9:2312.
23. Li BH, Garstka MA, Li ZF. Chemokines and their receptors promoting the recruitment of myeloid-derived suppressor cells into the tumor. Mol Immunol 2020;117:201-15.
24. Raimondo S, Saieva L, Vicario E et al. Multiple myeloma-derived exosomes are enriched of amphiregulin (AREG) and activate the epidermal growth factor pathway in the bone microenvironment leading to osteoclastogenesis. J Hematol Oncol 2019;12:2.
25. Romano A, Conticello C, Cavalli M et al. Immunological dysregulation in multiple myeloma microenvironment. Biomed Res Int 2014;2014:198539.
26. Pausch TM, Aue E, Wirsik NM et al. Metastasis-associated fibroblasts promote angiogenesis in metastasized pancreatic cancer via the CXCL8 and the CCL2 axes. Sci Rep 2020;10:5420.
27. Bardhan K, Paschall AV, Yang D et al. IFNgamma Induces DNA Methylation-Silenced GPR109A Expression via pSTAT1/p300 and H3K18 Acetylation in Colon Cancer. Cancer Immunol Res 2015;3:795-805.
28. Botta C, Di Martino MT, Ciliberto D et al. A gene expression inflammatory signature specifically predicts multiple myeloma evolution and patients survival. Blood Cancer J 2016;6:e511.
29. Zhang Y, Zhou L, Gu G et al. CXCL8(high) inflammatory B cells in the peripheral blood of patients with biliary atresia are involved in disease progression. Immunol Cell Biol 2020;98:682-92.
30. Jones RJ, Singh RK, Shirazi F et al. Intravenous Immunoglobulin G Suppresses Heat Shock Protein (HSP)-70 Expression and Enhances the Activity of HSP90 and Proteasome Inhibitors. Front Immunol 2020;11:1816.
31. Hanahan D, Weinberg RA. Hallmarks of cancer: the next generation. Cell 2011;144:646-74.
32. Wojdyla T, Mehta H, Glaubach T et al. Mutation, drift and selection in single-driver hematologic malignancy: Example of secondary myelodysplastic syndrome following treatment of inherited neutropenia. PLoS Comput Biol 2019;15:e1006664.

33. Vandyke K, Zeissig MN, Hewett DR et al. HIF-2alpha Promotes Dissemination of Plasma Cells in Multiple Myeloma by Regulating CXCL12/CXCR4 and CCR1. Cancer Res 2017;77:5452-63.
34. Bouyssou JM, Ghobrial IM, Roccaro AM. Targeting SDF-1 in multiple myeloma tumor microenvironment. Cancer Lett 2016;380:315-8.
35. Choi DS, Stark DJ, Raphael RM et al. SDF-1alpha stiffens myeloma bone marrow mesenchymal stromal cells through the activation of RhoA-ROCK-Myosin II. Int J Cancer 2015;136:E219-29.
36. Subat S, Mogushi K, Yasen M, Kohda T, Ishikawa Y, Tanaka H. Identification of genes and pathways, including the CXCL2 axis, altered by DNA methylation in hepatocellular carcinoma. J Cancer Res Clin Oncol 2019;145:675-84.
37. Lentini G, Fama A, Biondo C et al. Neutrophils Enhance Their Own Influx to Sites of Bacterial Infection via Endosomal TLR-Dependent Cxcl2 Production. J Immunol 2020;204:660-70.
38. Subat S, Mogushi K, Yasen M, Kohda T, Ishikawa Y, Tanaka H. Identification of genes and pathways, including the CXCL2 axis, altered by DNA methylation in hepatocellular carcinoma. J Cancer Res Clin Oncol 2019;145:675-84.
39. Yang Y, Zhou X, Li Y et al. CXCL2 attenuates osteoblast differentiation by inhibiting the ERK1/2 signaling pathway. J Cell Sci 2019;132:jcs230490.
40. Marchica V, Toscani D, Corcione A et al. Bone Marrow CX3CL1/Fractalkine is a New Player of the Pro-Angiogenic Microenvironment in Multiple Myeloma Patients. Cancers (Basel) 2019;11:321.
41. Wada A, Ito A, Iitsuka H et al. Role of chemokine CX-3CL1 in progression of multiple myeloma via CX3CR1 in bone microenvironments. Oncol Rep 2015;33:2935-9.
42. Karnezis T, Farnsworth RH, Harris NC et al. CCL27/CCL28-CCR10 Chemokine Signaling Mediates Migration of Lymphatic Endothelial Cells. Cancer Res 2019;79:1558-72.
43. Korbecki J, Kojder K, Siminska D et al. CC Chemokines in a Tumor: A Review of Pro-Cancer and Anti-Cancer Properties of the Ligands of Receptors CCR1, CCR2, CCR3, and CCR4. Int J Mol Sci 2020;21:8412.
44. Xu R, Li Y, Yan H et al. CCL2 promotes macrophages-associated chemoresistance via MCPIP1 dual catalytic activities in multiple myeloma. Cell Death Dis 2019;10:781.
45. Yin X, Han S, Song C et al. Metformin enhances gefitinib efficacy by interfering with interactions between tumor-associated macrophages and head and neck squamous cell carcinoma cells. Cell Oncol (Dordr) 2019;42:459-75.
46. Stellato C, Collins P, Ponath PD et al. Production of the novel C-C chemokine MCP-4 by airway cells and comparison of its biological activity to other C-C chemokines. J Clin Invest 1997;99:926-36.
47. Xia M, Hu S, Fu Y et al. CCR10 regulates balanced maintenance and function of resident regulatory and effector T cells to promote immune homeostasis in the skin. J Allergy Clin Immunol 2014;134:634-44.
48. Heath H, Qin S, Rao P et al. Chemokine receptor usage by human eosinophils. The importance of CCR3 demonstrated using an antagonistic monoclonal antibody. J Clin Invest 1997;99:178-84.
49. Du W, Shen T, Li H et al. Urinary NGAL for the diagnosis of the renal injury from multiple myeloma. Cancer Biomark 2017;18:41-6.